A Novel Topology for Enhancing the Low Voltage Ride through Capability for Grid Connected Wind Turbine Generators

R. A. Ibrahim, M.S. Hamad, Y.G. Dessouky
Electrical and Control Engineering Department
Arab Academy for Science and Technology & Maritime Transport
Alexandria, (*Egypt*)

B.W. Williams
Electronics and Electrical Engineering Department
Strathclyde University
Glasgow, (*United Kingdom*)

Abstract— **Energy shortage and environmental pollution have led to the increasing demand of using renewable sources for electricity production. Currently, power generation from wind energy systems (WES) is of global significance and will continue to grow during the coming years leading to concerns about power system stability where wind farms replace conventional generating technologies that use fossil fuels as the primary energy source. One of these concerns is Low-Voltage Ride-Through (LVRT). In this paper, a novel topology based on the use of magnetic amplifier for enhancing the LVRT capability for grid connected permanent magnet synchronous generators (PMSG) is presented. The system performance is investigated using Matlab.**

Keywords-component; permanent magnet synchronous generator, low voltage ride through, wind energy grid connection, magnetic amplifier, renewable energy

LIST OF SYMBOLS

C_p	Performance coefficient of wind turbine
f	Supply frequency, (Hz)
i_b	Boost converter inductor current, (A)
i_{dg}, i_{qg}	*dq* PMSG stator current components, (A)
i_a, i_b, i_c	Three phase grid currents, (A)
i_d, i_q	*dq* axis components of grid currents, (A)
i_d^*, i_q^*	*dq* reference grid current components, (A)
i_s	PMSG supply current, (A)
i_c	Magnetic amplifier control winding current, (A)
I_{inv}	Inverter IGBT current, (A)
I_{rec}	Rectifier diode current, (A)
L_f	Booster inductance, (H)
L_d, L_q	PMSG *dq* axis inductances, (H)
P_w	Power absorbed by windmill, (W)
P_{Grid}, Q_{Grid}	Grid active and reactive power, (W, VAR)
P_{Gen}, Q_{Gen}	PMSG active and reactive power, (W, VAR)
R_a	Stator armature resistance, (Ω)
R	windmill blade radius, (m)
T_e	Electromagnetic torque, (N.m)
V	Wind velocity (m/s)
V_{inv}	Inverter IGBT voltage, (V)
v_b	Input capacitor voltage of boost converter, (V)
v_{dc}	DC link capacitor voltage, (V)
V_{rec}	Rectifier diodes reverse voltage, (V)
v_a, v_b, v_c	Three phase grid voltages, (A)
β	Blade pitch angle (*BPA*), degree
δ	Load angle, between *q*-axis and phase 'a' voltage, (rad)
φ_f	Permanent magnet flux linkage, (Wb)
φ_d, φ_q	*dq* axis flux-linkages, (Wb)
θ	Phase angle of grid voltage, (degree)
λ	Tip-speed ratio (*TSR*)
ρ	Air density
ω	Electrical rotor angular speed, (rad/s)

I. INTRODUCTION

The increasing consumption of the traditional fossil energy raises problems such as global warming, pollution and energy security. Renewable energy sources are the most promising alternative energy in future. With the increasing penetration of wind energy and the improvement of its technology make it important to carefully reconsider the operating characteristics of wind farms, especially during grid fault conditions. Previously, disconnection of distributed generators (DGs) if one of the parameters (e.g. voltage, frequency, etc.) was beyond or below the permissible band was not a problem as the installed DG capacity was low. However, with installed mega watt (MW) of wind power, disconnection of the DG is no longer valid. Disconnection of many wind turbines (WT) during fault and evoked loss of a large share of generation can be dangerous for the stability of the power system operation. Thus, new connection requirements for DG units have been introduced by many system operators [1]. For these reasons, wind turbines are expected to behave like conventional synchronous generators during voltage dips, remaining connected and supplying reactive power during and after the voltage dip. For example, the LVRT requirement for the UK electrical grid is shown in figure (1) [2], where the wind turbine has to remain connected to the network for grid faults that last up to 140 ms and upon the restoration of voltage to 90% of nominal.

978-1-4673-0803-8/12/$31.00 ©2012 IEEE

During normal operation of WT and with the absence of grid voltage dips, the wind energy conversion system (WECS) extracts maximum power from the wind regardless of wind speed. The turbine controller achieves the maximum power point tracking (MPPT) algorithm [3-5]. The extracted power passes through stages of power electronic conversions and connected to the grid at the end. When a network fault occurs, the wind turbine DC link voltages rise rapidly as the WT grid side converter is prevented from transmitting the active power coming from the generators. Therefore, to maintain the wind turbine DC link voltage below its upper limit, either dissipating the excess power or reducing the generator power is mandatory.

Methods for LVRT capability enhancement and overcoming the rise in DC link voltage vary according to the turbine variables and utility grid variables. To enhance the LVRT capability for WT, blade pitch angle control can be used as in [6] through shifting the WT blades from an angle where it extracts maximum power to another angle of attack, thus reducing the amount of power being extracted from the wind and compensating the rise in the DC link voltage. Another suggested solution is to oversize the DC link capacitor to compensate for the DC link voltage rise during grid dips as in [7]. Active crow bar technique is considered one of the mostly used solutions for LVRT. By the insertion of a resistor in the dc link controlled by a power electronic switch, excess energy is dissipated and a balanced power flow is restored [8]. Other methods for LVRT improvement can be through de-loading of the wind turbine as demonstrated in [9] by the proper control of generator side converter, grid side converter control. The former controls the generator electromagnetic torque by controlling the generator armature current while the latter maintains the DC link voltage constant by controlling the grid side converter [10]. VAR and voltage compensation (shunt/series, shunt & series) has been one of the effective techniques in enhancing the LVRT capability on a larger scale such as wind farm level at the point of common coupling. VAR compensators employ the use of Static VAR Compensators (SVC), STATCOM, Magnetic Energy Recovery Switch (MERS), Dynamic Voltage Restorer (DVR) and Thyristor Controlled Series Capacitor (TCSC) [11-15].

This paper proposes a novel topology that can be used to enhance the LVRT capability for PMSG grid connected wind turbines. The topology is based on series voltage compensation using magnetic amplifiers. Magntic amplifier has been known for years and is used in varaiety of applications such as position control. It is a device which acts as a variable inductance if inserted between a source of emf and a load. Through proper control of its control winding current, magnetic amplifier will eventually act as a current limiter and a series voltage compensator at the event of transient voltage dip to enhance LVRT capability.

The basic principles of magnetic amplifiers design considerations are demonstarted to show the effectiveness of magnetic amplifier in reducing the DC link voltage rise as well as limiting the stresses on the power electronic converters in case of grid voltage dips.

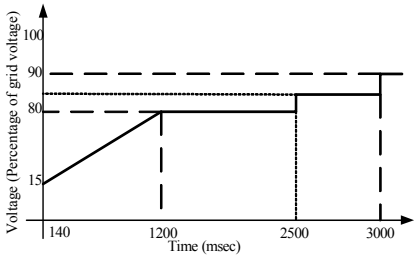

Figure 1: British Grid Code for Fault Ride Through

II. SYSTEM CONFIGURATION

A. *System Modeling:*

The WECS employed for grid connection of PMSG wind turbine is found in figure (2) which consists of the drive train, PMSG, diode bridge rectifier, boost converter circuit and a voltage source inverter (VSI). As mentioned earlier, MPPT is one of the essential features of grid connected WT. The techniques used for PMSG WT are vast and diverse. One of the oldest approaches is the tip speed ratio (TSR) technique, where the turbine pitch angle is regulated according to the measured wind speed. TSR's main disadvantage lies in the cost of the anemometers used as well as its low accuracy in the presence of wind gusts [16]. Hill climbing search technique (HCST) is another method for MPPT , where the PMSG shaft speed is perturbed in small steps while observing the wind turbine mechanical power [17, 18]. The disdavantage of HCST lies in the slow responces to wind changes as well as oscillation around the optimum point making the HCST suitable for small-scale WT. Finally, optimum relationship based (ORB) MPPT, is the most popular technique used with large scale WT. Lookup tables are recorded with stored values of optimal generator speed and the corresponding maximum power (or maximum torque) at various wind velocities. ORB requires system pre-knowledge and many field tests to obtain accurate optimal relation between system parameters [19-21].

In the absence of LVRT enhancement methodology, grid voltage dips can cause a serious rise in the DC link voltage which might lead to the destruction of the power converters. To demonstrate this effect, figure (2) shows the block diagram being used in the simulation analysis of a 1.5MWgrid connected PMSG WT whose parameters can be found in table (1). System description is presented in the following sections.

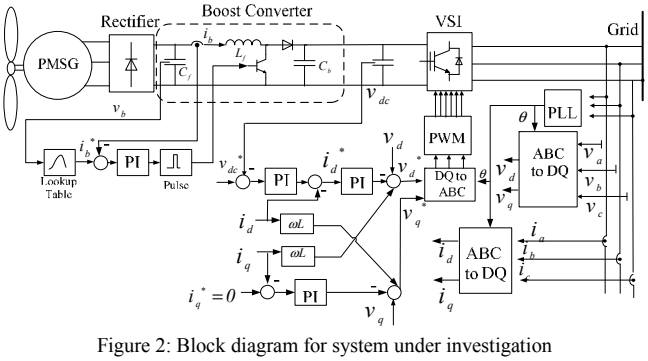

Figure 2: Block diagram for system under investigation

1) Wind Turbine Model:

The power absorbed by windmill from air, P_w , is given by (1)

$$P_w = \frac{1}{2}\rho\pi R^2 V^3 C_p \quad (1)$$

When wind velocity is invariable, the power P_w is directly proportional to Cp.

$$\lambda = \frac{\omega R}{V} \quad (2)$$

$$C_p = 0.73\left(\frac{151}{\lambda_1} - 0.58\beta - 0.2\beta^{2.14} - 13.2\right)e^{\frac{-18.4}{\lambda_1}} \quad (3)$$

$$\lambda_1 = \frac{1}{\left(\frac{1}{\lambda - 0.02\beta} - \frac{0.08}{\beta^3 + 1}\right)} \quad (4)$$

Table 1: PMSG DATA [22]

Parameter	Value
Base power (MVA)	1.5
Base voltage (V)	690/√3
Base frequency (Hz)	11.5
Pole pairs of PMSG	40
PMSG inertia constant (pu)	0.5
Shaft stiffness (pu)	2
Rated generator torque (pu)	1
Rated generator line voltage (pu)	1
Generator inductance in the *d* frame (pu)	0.7
Generator inductance in the *q* frame (pu)	0.7
Generator stator resistance (pu)	0.01
Flux of the permanent magnets (pu)	0.9

As it can be noticed from (1)- (4), Cp varies as a function of both the TSR and the BPA. For every fixed BPA there is a corresponding $Cp - \lambda$ curve each has a peak Cp value corresponding to an optimum TSR. Maximum Cp is achieved at optimized rotational speed ω when β is equal to zero [10].

2) Permanent Magnet Synchronous Generator (PMSG):

Variable speed direct driven PMSG wind turbines have gained increasing interest over the externally excited synchronous machine due to a significant reduction in magnet prices and magnetic material characteristics improvement. Variable-speed operation of a WTES has many advantages such as rapid response to wind speed & torque variation, causing less wear and tear on the tower and other components in the drive train. Variable-speed systems can also increase the production of the energy and reduce the fluctuation of the power injected into the grid [23]. A *dq* model of PMSG has been developed using equations (5)- (7) found in [24].

$$v_d = R_a i_d + L_d \frac{\partial i_d}{dt} - \omega L_q i_q \quad (5)$$

$$v_q = R_a i_q + L_q \frac{\partial i_q}{dt} + \omega\varphi_f + \omega L_d i_d \quad (6)$$

$$T_e = \frac{3}{2}\rho i_q\left(\left(L_q - L_d\right)i_d + \varphi_f\right) \quad (7)$$

3) Three phase Diode Rectifier

For grid connected PMSG WT, generator's output voltage and frequency must be maintained within certain values to ensure proper grid interconnection. Since the PMSG output power is of fluctuating nature due to wind speed variability, power electronic converters are utilized to overcome such problems. Three phase diode bride rectifier has been used for AC-DC conversion of the generator output power.

4) Boost Converter

A boost converter has been added in the DC link to extract maximum power from the WT at any given wind speed as well as expand its scope of low speed operation. Using the ORB technique for MPPT, an optimal relation between booster converter inductor current i_b versus boost converter capacitor DC voltage v_b can be found [19] .This is true as v_b is proportional to the PMSG electromotive force, and the latter is proportional to the rotational speed. By sensing the DC voltage v_b and using the optimal relation between v_b and i_b , the chopper circuit extracts maximum power from the PMSG at any wind speed. Although this method requires many offline tests, it accounts for turbine effeciency and takes into consideration the total power converters losses.

5) Three phase PWM VSI

A current regulated PWM VSI maintains the boost converter output voltage (DC link voltage) at a fixed value by balancing the input and output power at the dc-link. The PWM VSI employs two control loops, the inner loop is for the grid current control while the outer loop is for the DC link voltage control. Decoupling the grid currents in the *dq* axis frames provides means for controlling the active grid current at unity power factor by setting the *q*-axis current to zero.

B. System Behavior for Voltage Dips and LVRT Capability:

The system in figure (2) has been studied for several grid voltage dips of 30%, 60% and 90% at 0.4, 0.8 and 1.2 s to demonstrate the impact on the system elements and the simulation results are shown in figures (3)- (9). All simulation results used in the analysis are carried out using Simulink-Matlab software. During the voltage dip incidance, the grid power will fall in response to the voltage dip while the PMSG will continue to extract maximum power from the wind turbine through the boost converter as seen from figures (5) and figure (6). Since the grid power has fallen to very low value, the power extracted from the wind will be transformed into stored energy in the DC link capacitor. As for figure (3) and figure (7), grid voltage dips cause a rapid rise in the DC link voltage, reaching almost to double the normal voltage which the capacitor can tolerate when a 90% dip occurs. The rise level depends on the capacitor size , dip voltage duration and network effective impedance, which can be more than just double the normal capacitor operating voltage. The DC link voltage rise accompanies more voltage stresses on the PWM VSI as seen in figure (7) while the diode bridge rectifier suffers from neither voltage nor current stress as found in figure (8) and figure (9).

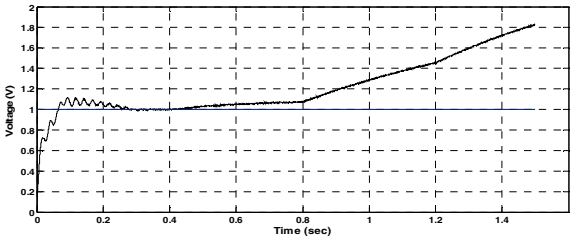

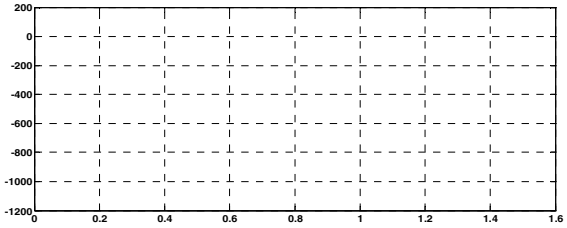

Figure 3: DC link voltage for 30%, 60% and 90% voltage dip

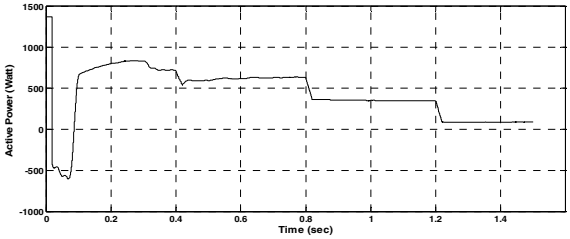

Figure 4: PMSG active power for 30%, 60% and 90% voltage dip

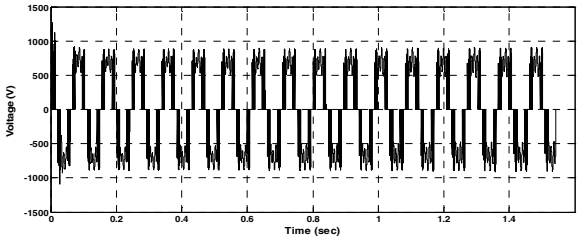

Figure 5: PMSG terminal voltage for 30%, 60% and 90% voltage dip

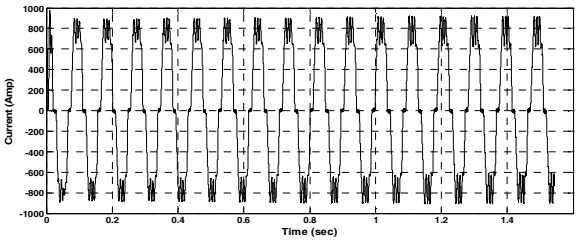

Figure 6: PMSG supply current for 30%, 60% and 90% voltage dip

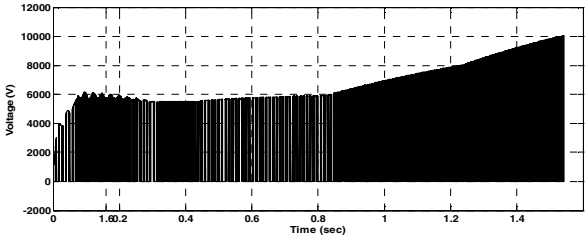

Figure 7: IGBT switch voltage for 30%, 60% and 90% voltage dip

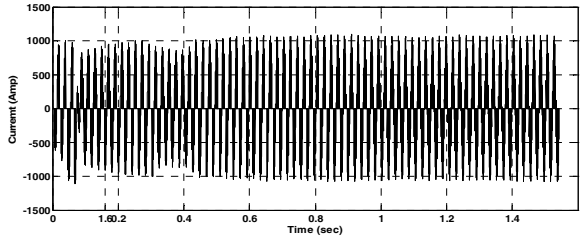

Figure 8: IGBT switch current for 30%, 60% and 90% voltage dip

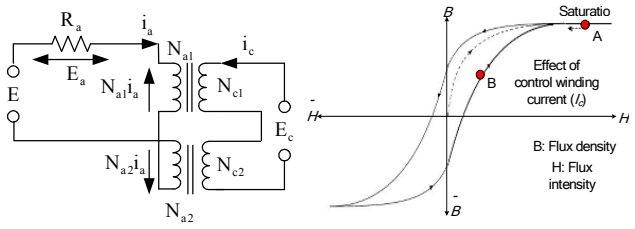

Figure 10: Connection and *B-H* curve of a magnetic amplifier

On the other hand, if the coupling co-efficient is small, then a large current signal is required to polarize the core and the power level at the control winding would be reasonably high[32]. Splitting the load winding into two coils connected in series opposition neutralizes the transformer action. Another modification can be made to the circuit is to include a diode in series with each of the two main windings. In this case, full utilization of the full alternating current would give higher efficiency and better waveform and reduce the time delay that can reach up to half cycle of the supply frequency.

B. Magnetic Amplifiers and LVRT Capability Enhancement:

The magnetic amplifier can be used as a method of series compensation. Changing of its control winding current changes the main winding effective impedance, thus the magnetic amplifier acts as a variable inductance if inserted between a source of emf and a load. To validate this idea, the magnetic amplifier have been used and tested for LVRT enhancement as seen in figure (11). In this configuration, each of the three phases of the PMSG is split into two windings as to avoid demagnetization of the magnetic amplifier in the negative half cycle of the supply voltage. Each winding is connected in series with a rectifying diode which helps the magnetic amplifier cores to reach saturation faster [32]. Six magnetic amplifiers have been used in the following analysis, each rating

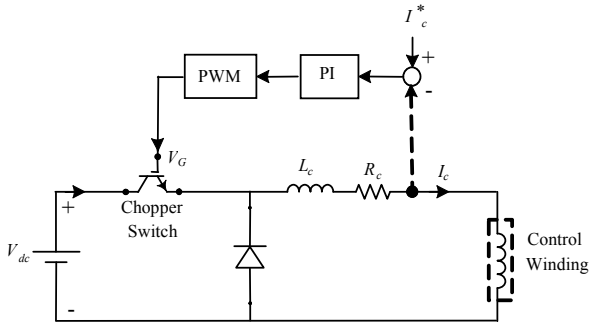

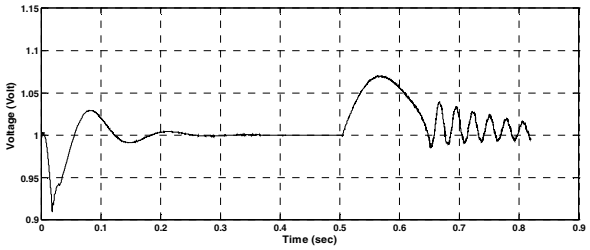

Figure 11: DC link voltage at 90% voltage dip with magnetic amplifier

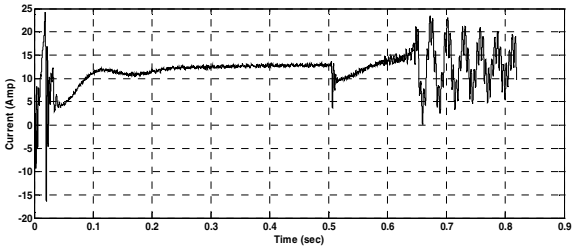

Figure 12: DC link current at 90% voltage dip with magnetic amplifier

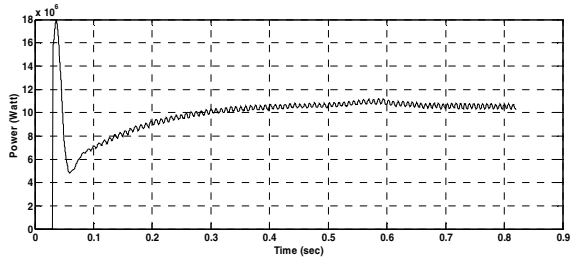

Figure 13: PMSG active power at 90% voltage dip with magnetic amplifier

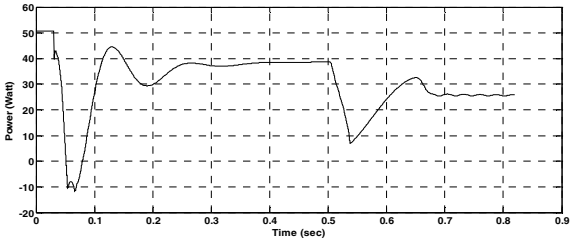

Figure 14: Grid power at 90% voltage dip with magnetic amplifier added

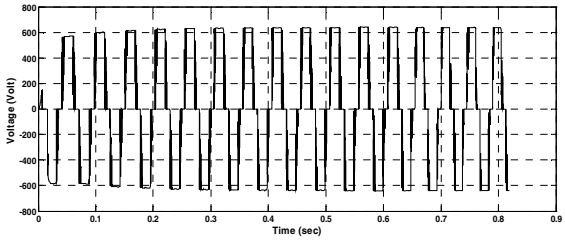

Figure 15: PMSG terminal voltage at 90% voltage dip with magnetic amplifier

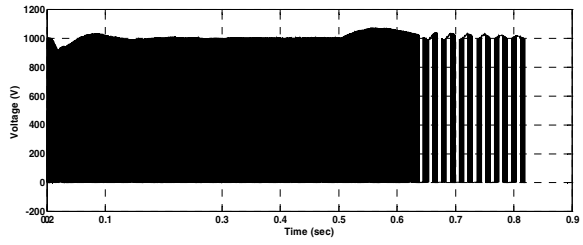

Figure 16: IGBT switch voltage at 90% voltage dip with magnetic amplifier

IV. CONCLUSION

Enhancement of low voltage ride through capability for wind turbines is becoming one of the most important issues related to the utilization and connection of wind turbines to the electrical grid. Several techniques have been adopted in literatures that ensure that grid codes are being complied in the event of grid voltage dips which, not only ensure the stability of the electrical grid post the voltage dip, but also ensure the safety of wind farm during the dip event. A novel topology based on using magnetic amplifiers in the event of grid voltage dips is demonstrated. Simulation results show that magnetic amplifier can be used to enhance the LVRT capability for direct driven PMSG WES. The application extends for the use with DFIG wind energy systems as well.

V. REFERENCES

[1] B. M. Buchholz, *et al.*, "Dynamic simulation of renewable energy sources and requirements on fault ride through behavior," *IEEE Power Engineering Society General Meeting,* 2006.

[2] M. Tsili and S. Papathanassiou, "A review of grid code technical requirements for wind farms," *IET Transaction on Renewable Power Generation,* vol. 3, p. 308, 2009.

[3] C.T. Pan and Y.L. Juan, "A novel sensorless mppt controller for a high-efficiency microscale wind power generation system," *IEEE Transaction on Energy Conversion,* vol. 25, pp. 207-216, 2010.

[4] S. Morimoto, *et al.*, "Sensorless output maximization control for variable-speed wind generation system using ipmsg," *IEEE Transaction on Industry Applications,* vol. 41, pp. 60-67, Jan./Feb. 2005.

[5] V. Cecconi, *et al.*, "Active power maximizing for wind electrical energy generating systems moved by a modular multiple blade fixed pitch wind turbine," *IEEE International Symposium on Power Electronics, Electrical Drives, Automation and Motion, SPEEDAM'08*, pp. 1460 - 1465, 2008.

[6] N.P.W. Strachan and D. Jovcic, "Dynamic modeling, simulation and analysis of an offshore variable-speed directly-driven permanent-magnet wind energy conversion and storage system (wecss)," *presented at the OCEANS 2007 - Europe*, pp. 1-6, 2007.

[7] J. F. Conroy and R. Watson, "Low-voltage ride-through of a full converter wind turbine with permanent magnet generator," *IET Transaction on Renewable Power Generation,* vol. 1, no.3, pp. 182 - 189, 2007.

[8] W. Zhang, *et al.*, "Analysis of the by-pass resistance of an active crowbar for doubly-fed induction generator based wind turbines under grid faults " *IEEE International Conference on Electrical Machines and Systems, ICEMS'08*, pp. 2316 - 2321, 2008.

[9] G. Ramtharan, *et al.*, "Fault ride through of fully rated converter wind turbines with ac and dc transmission systems," *IET Transaction on Renewable Power Generation,* vol. 3, no.3, p. 426, 2009.

[10] Y. Xiao-ping, *et al.*, "Low voltage ride-through of directly driven wind turbine with permanent magnet synchronous generator," *IEEE Power and Energy Engineering Conference, APPEEC'09*. pp. 1-5, 2009.

[11] M.H. Ali and B. Wu, "Comparison of stabilization methods for fixed-speed wind generator systems," *IEEE Transaction on Power Delivery* vol. 25, no.1, pp. 323-331, Jan. 2010.

[12] G. Wenming, *et al.*, "A survey on recent low voltage ride-through solutions of large scale wind farm," *IEEE Power and Energy Engineering Conference, APPEEC'11,* pp. 1-5, 2011.

[13] O. Abdel-Baqi and A. Nasiri, "Series voltage compensation for dfig wind turbine," *IEEE Transaction on Energy Conversion* vol. 26, no.1, pp. 272-280, 2011.

[14] S. Zhang, *et al.*, "Advanced control of series voltage compensation to enhance wind turbine ride-through," in *IEEE Transaction on Power Electronics*, vol.27, no.2, pp. 763 - 772, 2011.

[15] S. Raphael and A. Massoud, "Unified power flow controller for low voltage ride through capability of wind-based renewable energy grid-connected systems " *IEEE 8th International Multi-Conference on Systems, Signals and Devices*, pp.1-6, 2011.

[16] E. Koutroulis and K. Kalaitzakis, "Design of a maximum power tracking system for wind-energy-conversion applications," *IEEE Transactions on Industrial Electronics,*, vol. 53, no.2, pp. 486-494, 2006.

[17] K. Raza, *et al.*, "A novel algorithm for fast and efficient maximum power point tracking of wind energy conversion systems," IEEE 18th *International Conference on Electrical Machines, ICEM*, pp. 1-6, 2008.
[18] I. K. Buehring and L. L. Freris, "Control policies for wind-energy conversion systems," *IEE Proceedings on Generation, Transmission and Distribution,* vol. 128, no.5, pp. 253-261, 1981.
[19] M. Adam, *et al.*, "Architecture complexity and energy efficiency of small wind turbines," *IEEE Transaction on Industrial Electronics* vol. 54, no.1, pp. 660-670, 2007.
[20] K. Tan and S. Islam, "Optimum control strategies in energy conversion of pmsg wind turbine system without mechanical sensors," *IEEE Transactions on Energy Conversion,* vol. 19, no.2, pp. 392-399, 2004.
[21] P. Ching-Tsai and J. Yu-Ling, "A novel sensorless mppt controller for a high-efficiency microscale wind power generation system," *IEEE Transaction on Energy Conversion* vol. 25, no.1, pp. 207-216, 2010.
[22] H. Geng, *et al.*, "Unified power control for pmsg-based wecs operating under different grid conditions," *IEEE Transaction on Energy Conversion* vol. 26, no.3, pp. 822 - 830 2011.
[23] Z. Chen, *et al.*, "A review of the state of the art of power electronics for wind turbines," *IEEE Transactions on Power Electronics* vol. 24, no.8, pp. 1859-1875, 2009.
[24] P. C. Krause, *et al.*, *Analysis of electric machinery and drive systems*: John Wiely and Sons, INC. Publication, 2002.
[25] C. W. Lufcy, "A survey of magnetic amplifiers," *Proceedings of the IRE* pp. 404-413, 1955.
[26] R. Feinberg, "A review of transductor principles and applications," *IEE Proceedings on Power Engineering - Part II: ,* vol. 97, no.57, pp. 628-644, 1950.
[27] H. M. Gale and P. D. Atkinson, "A theoretical and experimental study of the series connected magnetic amplifier," *Journal of the Institution of Electrical Engineers,* vol.1949, no.6, pp. 99-114, 1949.
[28] C. S. Hudson, "A theory of the series transductor," *IEE Proceedings on Power Engineering - Part II ,* vol. 97, no.60, pp. 751-755, 1950.
[29] K. C. Parton, *et al.*, "Superconducting power-system transductor," *IEE Proceedings on Generation, Transmission and Distribution,* vol. 128, no.4, pp. 235-242, 1981.
[30] A. U. Lamm, "Some fundamentals of a theory of the transductor or magnetic amplifier," Transactions of the American Institute of Electrical Engineers, vol. 66, no.1, pp. 1078-1085, 1947.
[31] Y. Shindo, *et al.*, "A magnetic amplifier using nanocrystalline soft magnetic material," *IEEE 8th International Conference on Power Electronics - ECCE'11* , pp. 1299 - 1306, 2011.
[32] E. H. F.-. Smith, *The theory and design of magnetic amplifiers*: Chapman and Hall 1966.